1 **_Arabidopsis_ Topless-related 1 mitigates physiological damage**

2 **and growth penalties of induced immunity**

3 Thomas Griebel[1,2*], Dmitry Lapin[1,3*], Federica Locci[1], Barbara Kracher[1,a], Jaqueline

4 Bautor[1], Jingde Qiu[1,b], Lorenzo Concia[4], Moussa Benhamed[4], Jane E. Parker[1,5]

5 1 - Department of Plant–Microbe Interactions, Max Planck Institute for Plant Breeding Research, Cologne,
6 Germany
7 2 - Dahlem Centre of Plant Sciences, Plant Physiology, Freie Universität Berlin, Berlin, Germany
8 3 - Plant-Microbe Interactions, Department of Biology, Faculty of Science, Utrecht University
9 4 - Institute of Plant Sciences Paris-Saclay (IPS2), CNRS, INRA, University Paris-Sud, University of Evry,
10 University Paris-Diderot, Sorbonne Paris-Cite, University of Paris- Saclay, Batiment, Orsay, France
11 5 - Cluster of Excellence on Plant Sciences (CEPLAS), Düsseldorf 40225, Germany
12 [a] Present address: Evotec (München) GmbH, Munich, Germany
13 [b] Present address: Department of Botany and Plant Sciences, University of California-Riverside, Riverside, CA
14 92521, USA
15 * - co-first authors
16
17 Correspondence to Jane E. Parker (parker@mpipz.mpg.de)

18
19

20 **Summary**

21 Transcriptional corepressors of the Topless family are important regulators of plant
22 hormone and immunity signaling. The lack of a genome-wide profile of their chromatin
23 associations limits understanding of transcriptional regulation in plant immune
24 responses. Chromatin immunoprecipitation with sequencing (ChIP-seq) was
25 performed on GFP-tagged Topless-related 1 (TPR1) expressed in _Arabidopsis thaliana_
26 lines with and without constitutive immunity dependent on _Enhanced Disease_
27 _Susceptibility 1_ (_EDS1_). RNA-seq profiling of pathogen-infected _tpl/tpr_ mutants and
28 assessments of growth and physiological parameters were employed to determine
29 TPL/TPR roles in transcriptional immunity and defense homeostasis. TPR1 bound to
30 promoter regions of ~1,400 genes and ~10% of the detected binding required _EDS1_
31 immunity signaling. A _tpr1 tpl tpr4_ (_t3_) mutant displayed mildly enhanced defense-
32 related transcriptional reprogramming upon bacterial infection but not increased
33 bacterial resistance. Bacteria or pep1 phytocytokine-challenged _t3_ plants exhibited,
34 respectively, photosystem II dysfunction and exacerbated root growth inhibition.
35 Transgenic expression of _TPR1_ restored the _t3_ physiological defects. We propose that
36 TPR1 and TPL-family proteins function in _Arabidopsis_ to reduce detrimental effects
37 associated with activated transcriptional immunity.
38

Introduction

39

40 Plant disease resistance to pathogenic microbes is mediated by cell-surface and

41 intracellular immune receptors (Cui *et al.*, 2015; Jones *et al.*, 2016; Albert *et al.*, 2020).

42 Extracellular leucine-rich repeat (LRR) domain receptors recognize pathogen-

43 associated molecular patterns (PAMPs) or host-secreted phytocytokine peptides to

44 confer pattern-triggered immunity (PTI) (Albert *et al.*, 2020). Intracellular nucleotide-

45 binding domain/LRR (NLR) immune receptors intercept pathogen virulence factors

46 (called effectors) after their delivery to host cells to produce effector-triggered immunity

47 (ETI). These two receptor systems cooperate to provide robust resistance, often

48 associated with localized host cell death (Ngou *et al.*, 2021; Yuan *et al.*, 2021).

49 All tested members of intracellular NLRs with N-terminal Toll and Interleukin-1 receptor

50 domains (referred to as TIR-NLRs or TNLs) and some cell membrane resident

51 receptor-like proteins (LRR-RP) signal via the nucleo-cytoplasmic immunity regulator

52 Enhanced Disease Susceptibility 1 (EDS1, (Fradin *et al.*, 2011; Lapin *et al.*, 2020; Pruitt

53 *et al.*, 2020; Dongus & Parker, 2021)). EDS1 forms exclusive, functional heterodimers

54 with its sequence-related partners Phytoalexin Deficient 4 (PAD4) and Senescence-

55 associated Gene 101 (SAG101, (Wagner *et al.*, 2013)). The EDS1 heterodimers

56 promote timely transcriptional upregulation of defenses in *Arabidopsis thaliana*

57 (hereafter *Arabidopsis*) which is necessary for the NLR-mediated bacterial resistance

58 (Cui *et al.*, 2018; Mine *et al.*, 2018; Bhandari *et al.*, 2019).

59 In *Arabidopsis*, WRKY family transcription factors (TFs) (Tsuda & Somssich, 2015;

60 Birkenbihl *et al.*, 2017; Zavaliev *et al.*, 2020), Systemic Acquired Resistance Deficient

61 1 (SARD1) and its homolog Calmodulin-Binding Protein 60-like g (CBP60g) (Sun *et*

62 *al.*, 2015; Ding *et al.*, 2020) have prominent roles in the early transcriptional

63 mobilization of defenses. As part of a network with WRKY TFs, CBP60g and SARD1

64 help to boost isochorismate synthase 1 (ICS1) biosynthesis and signaling of the

65 defense hormone salicylic acid (SA) in response to pathogen attack (Zhang *et al.*,

66 2010; Zhou *et al.*, 2018). These TFs are further transcriptionally induced salicylic acid

67 (SA) (Hickman *et al.*, 2019). A Myelocytomatosis (MYC) TF, MYC2, controls signaling

68 by the defense hormone jasmonic acid (JA, (Lorenzo *et al.*, 2004; Zander *et al.*, 2020))

69 that, together with SA, contributes to PTI and ETI (Tsuda *et al.*, 2009; Liu *et al.*, 2016;

70 Mine *et al.*, 2018). The SA- and JA-triggered signaling branches can antagonize each

71 other, and bacteria employ effectors and coronatine, a structural mimic of JA, to

72 manipulate the hormonal crosstalk (Zheng *et al.*, 2012; Yang *et al.*, 2017). Coronatine-

73 mediated hijacking of JA pathways to dampen SA defense is blocked in *Arabidopsis*

74 ETI mediated by the TNL pair Resistant to *Ralstonia solanacearum* 1 (RRS1) and

75 Resistant to *Pseudomonas syringae* 4 (RPS4) (Sohn *et al.*, 2014; Cui *et al.*, 2018;

76 Bhandari *et al.*, 2019). In TNL[RRS1-RPS4] ETI, EDS1 enables a timely boost of the SA-

77 regulated transcription and suppression of the JA/MYC2-dependent gene expression

78 to counter bacterial growth (Cui *et al.*, 2018; Bhandari *et al.*, 2019).

79 Activated defenses can have detrimental effects on plant physiology and growth if they

80 are prolonged or constitutive (Todesco *et al.*, 2010; Ariga *et al.*, 2017; Caarls *et al.*,

81 2017; van Butselaar & Van den Ackerveken, 2020; Bruessow *et al.*, 2021). DNA

82 methylation and polycomb-dependent H3K27me3 marks, which deplete during plant

83 defense reactions (Dowen *et al.*, 2012; Yu *et al.*, 2013; Dvořák Tomaštíková *et al.*,

84 2021), help to limit *NLR* gene expression and growth penalties in uninfected plants

85 (Deng *et al.*, 2017; Zervudacki *et al.*, 2018; Huang *et al.*, 2021). However, the

86 processes of transcriptional restriction of potentially dangerous induced immunity

87 cascades after pathogen detection are still poorly understood.

88 Transcriptional corepressors form an additional layer of gene expression control in

89 eukaryotes. Plant Topless (TPL) and Topless-related (TPR) corepressors resemble

90 Groucho/Tup1 transcriptional corepressors and carry a WD40 repeat C-terminal region

91   and several N-terminal domains (Martin-Arevalillo *et al.*, 2017; Plant *et al.*, 2021). Via

92   the N-terminal domains, TPL/TPRs interact with ethylene response factor (ERF) -

93   amphiphilic repression (EAR) motifs present in multiple TFs (Szemenyei *et al.*, 2008;

94   Causier *et al.*, 2012) and inhibitors of hormone signaling (Pauwels *et al.*, 2010; Ke *et*

95   *al.*, 2015; Ma *et al.*, 2017; Martin-Arevalillo *et al.*, 2017; Kuhn *et al.*, 2020). Interactions

96   with EAR motifs enable recruitment of TPL/TPRs into oligomers and complexes with

97   histones, potentially reducing access of TFs to DNA (Ma *et al.*, 2017; Martin-Arevalillo

98   *et al.*, 2017). The CRA N-terminal domain in *Arabidopsis* TPL further contributes to an

99   oligomerization-independent mode of corepression, likely by preventing the

100   engagement of mediator subunits into active transcription complexes (Leydon *et al.*,

101   2021). Furthermore, TPL/TPRs interact with histone deacetylases, providing a

102   mechanism for the repression of gene expression via interfering with a transcription-

103   permissive chromatin state (Long *et al.*, 2006; Zhu *et al.*, 2010; Leng *et al.*, 2020).

104   Thus, several molecular mechanisms appear to assist TPL/TPRs corepressor activity.

105   TPL/TPRs were implicated in the regulation of plant immunity. First, oomycete and

106   fungal effectors target TPL/TPRs to promote host susceptibility (Harvey *et al.*, 2020;

107   Darino *et al.*, 2021). Second, mutating *TPL*, *TPR1* and *TPR4* in *Arabidopsis* or

108   silencing of *TPR1* in *Nicotiana benthamiana* compromised TNL receptor signaling and

109   an flg22 PAMP-triggered reactive oxygen species (ROS) burst (Zhu *et al.*, 2010; Zhang

110   *et al.*, 2019; Navarrete *et al.*, 2021). By contrast, *Arabidopsis TPR2* and *TPR3* were

111   identified as negative regulators of TNL Suppressor of Non-expressor of

112   Pathogenesis-related 1 (NPR1) constitutive 1 (SNC1)-conditioned autoimmunity

113   (Garner *et al.*, 2021). *Arabidopsis* TPR1 was found to associate with promoters of

114   genes that are downregulated in TNL[RRS1-RPS4] ETI (Bartsch *et al.*, 2006; Zhu *et al.*,

115   2010) and to repress expression of cyclic nucleotide-gated channel (*CNGC*) genes

116   also known as *Defense No Death 1* and *2* (*DND1/CNGC2* and *DND2/CNGC4*) (Zhu *et*

117   *al.*, 2010; Niu *et al.*, 2019). Since these *dnd* mutants show enhanced bacterial

118   resistance (Clough *et al.*, 2000; Jurkowski *et al.*, 2004), a picture emerged in which

119   TPR1 promotes TNL ETI by limiting expression of negative regulators of defense.

120   However, the lack of a genome-wide profile of TPL/TPR chromatin associations leaves

121   the functions of these corepressors in defense signaling unclear.

122   Here, using chromatin immunoprecipitation with sequencing (ChIP-seq), we examined

123   genome-wide *Arabidopsis* TPR1-chromatin associations that are conditional on or

124   independent of the *EDS1*-controlled immunity in *pTPR1:TPR1-GFP* expressing plant

125   lines. These data, combined with RNA expression profiles and physiological

126   phenotypes of wild type and *tpr1 tpl tpr4* (*t3*) mutant plants during bacterial infection,

127   suggest that the TPL family transcriptional corepressors mitigate deleterious effects of

128   induced immunity on plant health.

129

Materials and Methods

131   Plant materials and growth conditions

132   *Arabidopsis thaliana (L.) Heynh.* accession Col-0 *tpr1* single mutant, *tpr1 tpl tpr4* (*t3*)

133   triple mutant, *pTPR1:TPR1-GFP* Col-0 (*TPR1* Col), and *pTPR1:TPR1-HA* Col-0 stable

134   transgenic lines were described previously (Zhu *et al.*, 2010). *pTPR1:TPR1-GFP eds1-*

135   *2 (TPR1 eds1)* and *pTPR1:TPR1-GFP sid2-1* (*TPR1 sid2*) lines were generated by

136   crossing *TPR1* Col (Zhu *et al.*, 2010) with Col-0 *eds1-2* (Bartsch *et al.*, 2006) and Col-

137   0 *sid2-1* (Wildermuth *et al.*, 2001)*,* respectively. Complementation *tpr1 tpl tpr4*

138   *pTPR1:TPR1-GFP* lines were generated by floral dipping of *t3* with Agrobacteria

139   GV3101 pMP90 pSoup carrying *pCAMBIA1305-TPR1-GFP* (Zhu *et al.*, 2010). The

140   *coi1-41* mutant is described in (Cui *et al.*, 2018). A *myc2 myc3 myc4 sid2* mutant was

141   obtained by crossing a *myc2* (*jin2-1*) *myc3* (GK445B11) *myc4* (GK491E10) triple

142   mutant (Fernández-Calvo *et al.*, 2011) with *sid2-1*. *eds1-2* (Bartsch *et al.*, 2006) was

5

143   mainly used as *eds1* throughout the study, the *eds1-12* line (Ordon *et al.*, 2017) was

144   used in root growth inhibition and MAPK assays. Oligonucleotides for genotyping are

145   shown in Table S1. For bacterial infection assays, plants were grown under a 10 h light

146   period (~100 µmol/m^{2}sec) and 22°C day/20°C night temperature regime with 60%

147   relative humidity. For transformation and selection of combinatorial mutants, plants

148   were grown under 22 h light (~100 µmol/(m^{2}sec)) and a 22°C day/20°C night

149   temperature regime with 60% relative humidity.

150

151   Immunoblot analyses

152   For immunoblotting of TPR1-GFP, total protein extracts were prepared by incubating

153   liquid nitrogen-ground samples (~50 mg) in 2x Laemmli loading buffer (0.5 w/v) for 10

154   min at 95°C. Samples were centrifuged 1 min at 10,000 x g to remove cell debris prior

155   gel loading. Proteins were separated by 10% (v/w) SDS-PAGE (1610156, Bio-Rad)

156   and transferred to a nitrocellulose membrane (0600001, GE Healthcare Life Sciences).

157   α-GFP antibodies (no. 2956, Cell Signaling Technology, or no. 11814460001, Roche)

158   in combination with HRP-conjugated anti-rabbit or anti-mouse secondary antibodies

159   (A9044 or A6154, Sigma-Aldrich) were used. In MAPK3/6 phosphorylation assays,

160   seedlings were treated for 15 and 180 min with 200 nM pep1 or milliQ water (mQ,

161   mock) as a negative control. Proteins were extracted with a buffer containing 50 mM

162   Tris pH 7.5, 200 mM NaCl, 1 mM EDTA, 10 mM NaF, 2 mM sodium orthovanadate, 1

163   mM sodium molybdate, 10% (v/v) glycerol, 1 mM AEBSF, 0.1% Tween-20, 1 mM

164   dithiothreitol, 1x protease inhibitor cocktail (11836170001, Roche) and 1x phosphatase

165   inhibitor cocktail (4906845001, PhosStop). Extracts were resolved on 8% (v/w) SDS-

166   PAGE (1610156, Bio-Rad) and transferred onto a nitrocellulose membrane (0600001,

167   GE Healthcare Life Sciences). Primary antibody against phospho-p44/42 MAP kinase

168   (#9101, Cell Signaling Technologies) with HRP-conjugated anti-rabbit as secondary

6

169   antibody were used (A6154, Sigma-Aldrich). Signal detection was performed using

170   Clarity and Clarity Max luminescence assays (1705061 and 1705062, Bio-Rad). For

171   loading control, membranes were stained with Ponceau S (09276-6X1EA-F, Sigma-

172   Aldrich).

173

174   Salicylic acid quantitation

175   Quantification of free SA was done as described (Straus *et al.*, 2010) with a

176   chloroform/methanol/water extraction containing SA-d_4 (CS04-482_248, Campro

177   Scientific) as internal standard. After phase extraction, drying of polar phase, dissolving

178   in sodium acetate (pH 5.0), uptake in ethyl acetate/hexane (3:1), and derivatization, 1

179   μl sample was injected into a gas chromatograph coupled to a mass spectrometer (GC-

180   MS; Agilent) on a HP-5MS column (Agilent). Masses of SA-d_4 (*m/z* 271) and SA (*m/z*

181   267) were detected by selected ion monitoring and quantified using the Chemstation

182   software (Agilent).

183

184   Chlorophyll a fluorescence and chlorophyll quantification

185   Maximum quantum efficiency of PS-II (F_V/F_M) and the effective efficiency (ϕPSII) in

186   Col, *tpr1*, *t3*, and *eds1* leaves were determined after syringe-infiltration of *Pst* (OD_{600}=

187   0.005) by chlorophyll a fluorescence analysis using a MINI-PAM fluorimeter (Walz,

188   Effeltrich, Germany). Measurements of 3-4 leaves from independent plants were

189   performed at each timepoint in a randomized and rotating order between 1 and 3 pm

190   on days 0 - 4 after inoculation (10 am-11 am). Mock (10 mM $MgCl_2$)-infiltrated leaves

191   from different plants were measured as controls. To determine the maximum quantum

192   yield ($F_V/F_M = (F_M - F_0)/F_M$) (Baker, 2008), plants were first dark-acclimated for 20 min.

193   The operating PSII efficiency of photosystem II (ϕPSII =$(F_M'-F)/F_M'$) (Baker, 2008) was

194   determined with 12 saturating light flashes (~1300 μmol photons $m^{-2}s^{-1}$) at intervals of

7

195 20 s and an actinic light intensity of ~216 μmol photons m^{-2} s^{-1}. Data from three

196 independent experiments were combined, statistically analyzed using ANOVA and

197 Tukey's HSD test (α= 0.05) and plotted using the 'ggline' function in the 'ggpubr' R

198 package. Total leaf chlorophyll (a+b) content in the indicated genotypes was

199 determined at 3 d after syringe infiltration with *Pseudomonas syringae* pv. *tomato*

200 DC3000 bacteria (OD_{600}=0.005) or mock (10 mM $MgCl_2$) treatment. The chlorophyll

201 content in each sample was measured and calculated as a mean of three leaf discs

202 (diameter 8 mm) and analyzed according to (Porra *et al.*, 1989). Three independent

203 experiments were performed and pooled for the statistical analysis keeping experiment

204 as a factor in the ANOVA model (Tukey's HSD α=0.05; n=15).

205

206 Root growth inhibition assay

207 Root growth inhibition assays with pep1 and flg22 were performed as described

208 (Igarashi *et al.*, 2012) with adjustments. Seeds were surface-sterilized and transferred

209 into 48-well plates (one seed per well). Each well was supplied with 200 μl of 0.5x MS

210 (including vitamins and MES, pH5.4; M0255, Duchefa Biochemie) and 0,5% (w/v)

211 sucrose. The flg22 and pep1 peptides (GenScript; in mQ water) were administered at

212 final concentrations of 100 nM and 200 nM, respectively. Sterile mQ was added as a

213 mock control. Root lengths were measured at 10 days using ImageJ software. Root

214 growth inhibition (RGI) index was quantified as a ratio of root length of flg22 or pep1

215 treatment to mean of the mock-treated plants. Data from independent experiments

216 were combined, statistically analyzed using ANOVA (experiment as a factor) and

217 Tukey's HSD test.

218

219 Details on the TPR1-GFP ChIP- and RNA-seq procedures and data analysis as well

220 as bacterial growth and electrolyte leakage assays are in Supporting information

221 Methods S1.

222

223 **Results**

224 *Arabidopsis TPR1* **Col displays constitutive transcriptional immunity**

225 To investigate the role of TPR1 in plant immunity, we used an *Arabidopsis* Col-0 line

226 expressing TPR1-GFP under control of the 2 kb upstream sequence (*pTPR1:TPR1-*

227 *GFP*; hereafter *TPR1* Col) and displaying *EDS1-* and TNL *SNC1*-dependent

228 constitutive immunity and SA accumulation (Zhu *et al.*, 2010). We introduced a null

229 *eds1* (*eds1-2*) or *ics1* (*sid2-1*) mutation into *TPR1* Col to test TPR1-GFP functions

230 without *EDS1-* or *ICS1*/SA-dependent defenses (Wildermuth *et al.*, 2001; Bartsch *et*

231 *al.*, 2006). While TPR1-GFP accumulation was similar in all three lines (Fig. 1a),

232 stunting of 5-6-week-old *TPR1* Col plants was reduced in *TPR1 eds1* but not in *TPR1*

233 *sid2* ((Zhu *et al.*, 2010); Fig. 1b, S1a). Also, enhanced resistance of *TPR1* Col to

234 virulent *Pseudomonas syringae* pv. *tomato* DC3000 (*Pst*) bacteria (Zhu *et al.*, 2010)

235 was abolished in *TPR1 eds1* and partially compromised in *TPR1 sid2* plants ((Zhu *et*

236 *al.*, 2010), Fig. S1b). Both *TPR1 eds1* and *TPR1 sid2* plants accumulated low SA

237 compared to *TPR1* Col (Fig. S1c). These results suggest that constitutive defense in

238 *TPR1* Col is mediated primarily by an SA-independent branch of *EDS1* signaling,

239 consistent with the *TPR1* Col autoimmunity being dependent on TNL *SNC1* (Zhu *et al.*,

240 2010) promoting SA-independent signaling (Zhang *et al.*, 2003; Zhu *et al.*, 2010).

9
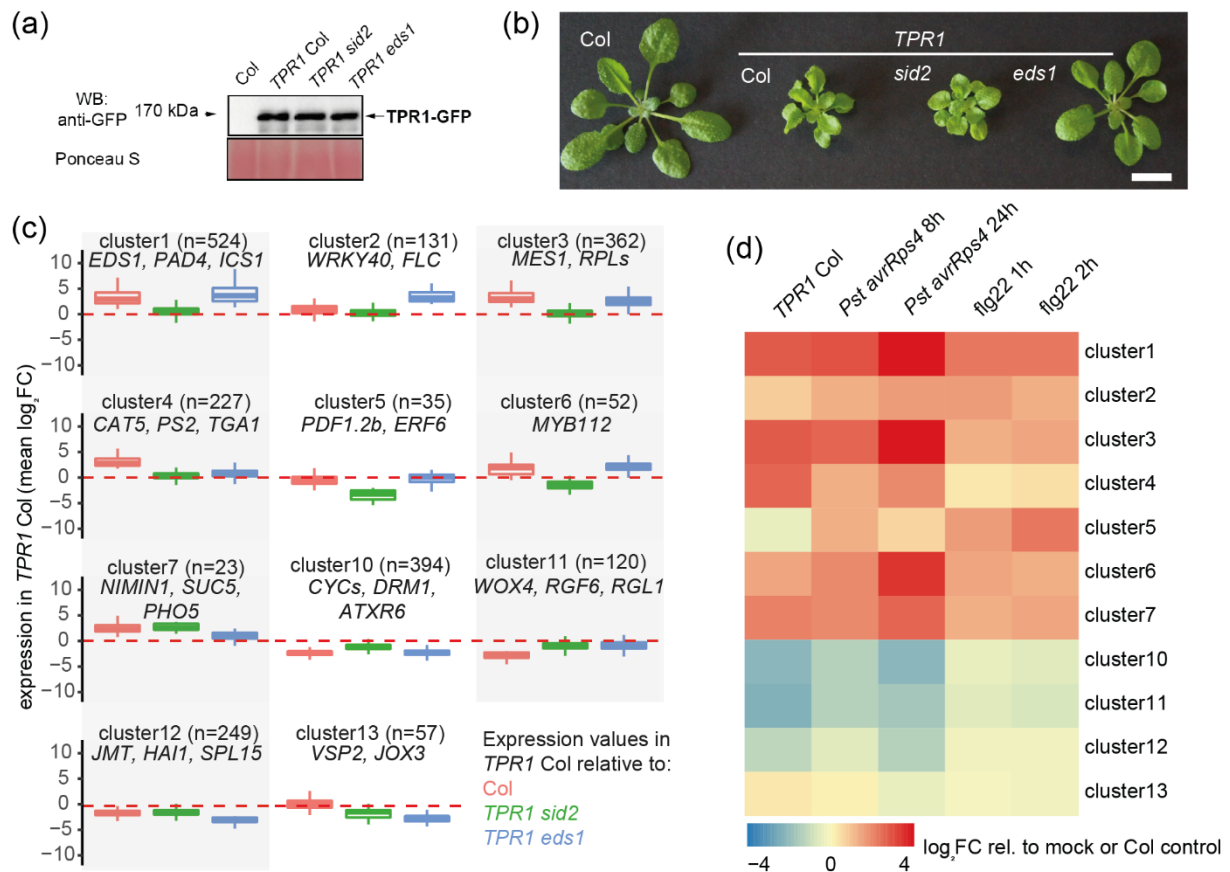
Fig. 1 Defense-related *EDS1*-dependent transcriptional reprogramming in *TPR1* Col line.
(a) TPR1-GFP steady-state accumulation in 5-6-week-old *Arabidopsis* Col-0 (Col), *sid2* and *eds1* mutant plants expressing *pTPR1:TPR1-GFP* (*TPR1* Col, *TPR1 sid2*, *TPR1 eds1*). The transgenic lines show similar levels of TPR1-GFP protein. Col was used as a negative control. Ponceau S staining indicates similar loading. The experiment was repeated three times with similar results. **(b)** Dwarfism in *TPR1* Col depends on functional *EDS1*. Col is shown on the left for comparison. Scale bar = 1 cm. **(c)** Boxplot representation of log$_2$-transformed relative expression values (fold change relative to *TPR1* Col) for clusters of genes differentially expressed in Col, *TPR1 eds1* and *TPR1 sid2*. Positive values reflect that the gene is stronger expressed in *TPR1* Col relative to Col (orange), *TPR1 sid2* (green) or *TPR1 eds1* (blue). Size of the cluster is given in parentheses. Names of selected genes from the clusters are in italics. **(d)** Relative mean expression for the gene clusters from (c) in *Arabidopsis* Col plants treated with *Pseudomonas syringae* pv. *tomato* DC3000 *avrRps4* or flg22 at the indicated time points. The values are mean log$_2$-transformed fold change expression values relative to mock or untreated Col plants (Birkenbihl *et al.*, 2017; Bhandari *et al.*, 2019).

241

242

243

10

244   The RNA-seq analysis of 5-6-week-old *TPR1* Col, *TPR1 sid2, TPR1 eds1* and wild

245   type Col plants showed that *EDS1* controlled 61% genes that are differentially

246   expressed between *TRP1* Col and Col (Table S2; 942/1549, $|log_2FC|≥2$, FDR≤0.05;

247   Fig. S1d). By contrast, the *sid2* mutation affected expression of only 10% differentially

248   expressed genes (DEGs) (Table S2; 153/1549, $|log_2FC|≥2$, FDR≤0.05). The 2,194

249   DEG between Col, *TPR1* Col, *TPR1 sid2* and *TPR1 eds1* fell into 13 groups in

250   hierarchical clustering of log_2-transformed gene expression changes (Fig. 1c, Table

251   S3). Cluster #1 with 524 genes induced in a *TPR1*/*EDS1*-dependent manner was

252   strongly enriched for gene ontology (GO) terms linked to *EDS1*- and SA-dependent

253   immune responses (Fig. 1c, Table S4). By contrast, cluster #10 with 394 genes

254   suppressed in *TPR1* Col (Figure 1c) was enriched for genes linked to the microtubule-

255   based dynamics and cell cycle regulation (Table S4). These data show that TPR1-GFP

256   constitutive immunity involves *EDS1*-dependent transcriptional reprogramming.

257   We tested whether the *TPR1* Col transcriptome aligns with gene expression changes

258   in PTI and ETI. For this, we cross-referenced DEGs in *TPR1* Col vs Col (Table S2)

259   with RNA-seq datasets for (i) Col inoculated with *Pst avrRps4* triggering an ETI[RRS1-

260   RPS4] (Bhandari *et al.*, 2019), and (ii) Col treated with the bacterial PAMP flg22 peptide

261   (Birkenbihl *et al.*, 2017) (Fig. 1d, S1e). Genes in clusters 1, 3, 4, 6 and 7 that were

262   upregulated in *TPR1* Col vs Col (Fig. 1c) were also induced by *Pst avrRps4* or flg22

263   treatments (Fig. 1d, S1e). Similarly, repressed clusters in *TPR1* Col (#10, #11, Fig. 1c)

264   were downregulated by these treatments (Fig. 1d, S1e). We concluded that the *TPR1*

265   Col line displays constitutive transcriptional immunity and that *TPR1* Col and *TPR1*

266   *eds1* are suitable backgrounds to measure immunity-dependent and independent

267   TPR1-chromatin associations.

268

269

11

270   **TPR1 binds to promoters of genes upregulated in immunity activated tissues**

271   We performed a ChIP-seq analysis on leaves of 5-6-week-old *TPR1* Col and *TPR1*

272   *eds1* plants (Fig. 2; Methods S1) using an input control for peak calling. A line

273   expressing *pTPR1:TPR1-HA* in Col showing constitutive immunity similarly to *TPR1*

274   Col (Zhu *et al.*, 2010) was included as an additional control for peak calling. In *TPR1*

275   Col, 1,531 TPR1-GFP chromatin binding sites corresponded to 1,441 genes (Table

276   S5). Most peaks (723/1531, 47%) mapped to 1 kb upstream gene sequences as

277   indicated by a metaplot analysis (Table S5, Fig. 2a,b) and consistent with the role of

278   TPR1 as a transcriptional corepressor acting at promoter regions (Niu *et al.*, 2019).

279   TPR1-bound genes showed enrichment of GO terms linked to defense and SA

280   signaling as well as developmental processes (Table S6, FDR≤0.05; Fig. S2-4), as

281   expected from the *TPR1* Col enhanced defense and perturbed growth phenotypes

282   (Fig. 1b,c).

283   In *TPR1 eds1* which lacks constitutive immunity (Fig. 1b,c, S1), we detected 614 TPR1-

284   GFP binding sites corresponding to 623 genes (Table S7; Fig. 2c). While the reduced

285   number of peaks in TPR1 *eds1* did not affect TPR1 distribution across genomic

286   fractions relative to *TPR1* Col (Fig. 2b,c, Table S7), the proportion of defense-related

287   GO terms enriched among TPR1-GFP bound genes plummeted in *TPR1 eds1* relative

288   to *TPR1* Col (Table S8). Hence, the TPR1-chromatin association with defense-related

289   genes appears to be enhanced in immune-activated shoot tissues. To assess this

290   further, we compared TPR1-chromatin associations in *TPR1* Col and *TPR1 eds1* using

291   a peak calling-independent method implemented in diffReps (Shen *et al.*, 2013). This

292   analysis showed that TPR1-GFP enrichment was stronger in *TPR1* Col relative to

293   *TPR1 eds1* at sites linked to 247 genes (G-test, 1.5 times difference, FDR≤0.05; Table

294   S9), suggestive of stronger TPR1 binding at these loci in immune-activated *TPR1* Col.

295　No ChIP peaks were called for 150 (61%) of these genes in *TPR1 eds1* (Table S5,

296　S7). Notably, 66 of the 247 differentially TPR1-bound genes (27%, including *ICS1*,

297　cysteine-rich receptor-like kinases and *WRKY* TFs (Fig. S2)) were more highly

298　expressed in *TPR1* Col compared to *TPR1 eds1* (Table S2, $\log_2$FC$\geq$1, FDR$\leq$0.05; Fig.

299　2d). Only ten genes from the above set of 247 (~4%) were downregulated in *TPR1* Col

300　compared to *TPR1 eds1* (Table S2, $\log_2$FC$\leq$1, FDR$\leq$0.05; Figure 2d). The TPR1 ChIP-

301　seq shows that TPR1 binds to ~1,400 genes mainly at promoter regions, and that

302　~11% of the detected TPR1 binding (150/1,441 genes) is conditional on *EDS1*-

303　dependent immunity.

304　We further tested whether *EDS1*-dependent TPR1-chromatin associations correlate

305　with transcriptional reprogramming during defense. A set of 247 genes with a stronger

306　TPR1-GFP signal in *TPR1* Col vs *TPR1 eds1* (Table S9) was generally upregulated in

307　RNA-seq after treatments with the bacterial PAMP flg22 and *Pst avrRps4* (Fig. 2e,

308　boxplots with orange shadowing). Conversely, expression of 74 genes with lower

309　TPR1-GFP enrichment in *TPR1* Col vs *TPR1 eds1* (Table S9) was unaltered in these

310　treatment (Fig. 2e, boxplots with green shadowing). These observations suggest that

311　there is increased TPR1 binding to a set of genes upregulated during bacterial PTI and

312　ETI.

313
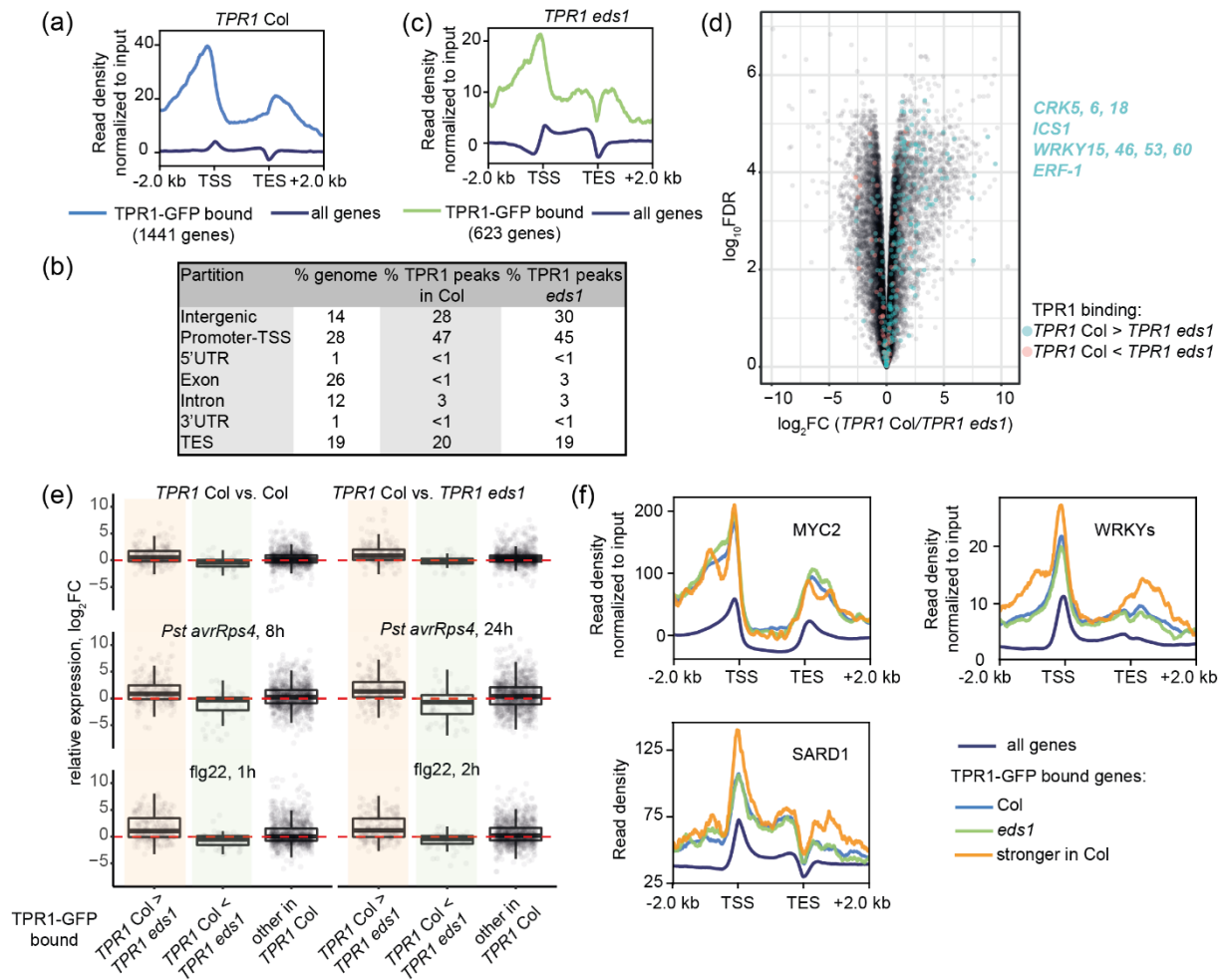
314

Fig. 2 *Arabidopsis* TPR1-chromatin association partially depends on *EDS1*-controlled immune signaling. (a-c) Metaplots of ChIP-seq TPR1-GFP enrichment profiles at the chromatin in *TPR1* Col (a) and *TPR1 eds1* (c) and distribution of TPR1 peaks over genome partitions (b). TPR1-GFP binds 1,441 genes in *TPR1* Col and 623 genes in *TPR1 eds1*. The ChIP-seq read density for TPR1-GFP was normalized to input via subtraction. The dark blue lines represent TPR1-GFP chromatin binding profiles averaged across all annotated genes in Arabidopsis (TAIR10). TSS = transcription start site, TES = transcription end site. **(d)** Volcano plot displaying the relationship between *EDS1*-dependent TPR1-chromatin associations and the *EDS1*-dependent gene expression regulation in *TPR1* Col. Significance of differences in the TPR1-GFP enrichment in *TPR1* Col and *TPR1 eds1* was assessed with diffReps (difference ≥1.5 times, G-test, FDR≤0.05). Genes with stronger enrichment of TPR1-GFP in *TPR1* Col than in *TPR1 eds1* (blue dots) tend to have higher gene expression in *TPR1* Col. Selection of these genes is shown in blue text. **(e)** log₂-scaled relative expression of TPR1-GFP-bound genes: *TPR1* Col vs Col, *TPR1* Col vs *TPR1 eds1*, treatments *Pseudomonas syringae pv. tomato* DC3000 (*Pst*) *avrRps4* (8 and 24 hpi vs 0 hpi) and flg22 (1 and 2 hpi vs 0 hpi) (Birkenbihl *et al.*, 2017; Bhandari *et al.*, 2019). Boxplots for genes showing stronger TPR1-GFP enrichment in *TPR1* Col vs *TPR1 eds1* are shaded in orange, and green shadowing highlights boxplots for genes with weaker TPR1-GFP signal in *TPR1* Col vs *TPR1 eds1*. Genes with higher TPR1-GFP enrichment in *TPR1* Col show transcriptional upregulation in PTI and *Pst avrRps4* infection. **(f)** Distribution of ChIP-seq signal for MYC2 (Wang *et al.*, 2019), WRKY (Birkenbihl *et al.*, 2018) and SARD1 (Sun *et al.*, 2015) transcription factors (TFs) across genes bound by TPR1-GFP in *TPR1* Col (light blue), *TPR1 eds1* (green) and genes bound stronger by TPR1-GFP in *TPR1* Col than in *TPR1 eds1* (orange). TF-chromatin binding profiles averaged across all annotated genes in Arabidopsis genome (dark blue) serve as a baseline. MYC2, WRKY TFs and SARD1 are strongly enriched in promoters of genes bound by TPR1-GFP *TPR1* Col and *TPR1 eds1*. ChIP-seq data for SARD1 (Sun *et al.*, 2015) did not have input samples and therefore were not normalized. ChIP-seq for MYC2 (Wang *et al.*, 2019) and WRKY TFs (Birkenbihl *et al.*, 2018) were normalized to the input via subtraction.

315

Genome-wide assessment of TPR1-chromatin binding reveals TPR1 and TPL targets

In the TPR1 ChIP-seq analysis, we detected TPR1 association to nine of twelve genes downregulated in TNL[RRS1-RPS4] ETI that were found as TPR1-bound targets in a previous ChIP-qPCR study using the *TPR1-HA* Col transgenic line (Zhu *et al.*, 2010). Genes with TPR1-GFP enrichment include *DND1* and *DND2* (Fig. S3) encoding CNGC2 and 4, respectively, which are required for calcium-dependent immunity responses in PTI and ETI (Clough *et al.*, 2000; Jurkowski *et al.*, 2004; Tian *et al.*, 2019). TPR1-GFP binding was not obviously altered in *TPR1 eds1* (Fig. S3), indicating immunity status-independent association of TPR1 with promoters of these nine genes. Since TPL/TPR proteins have redundant functions (Zhu *et al.*, 2010; Harvey *et al.*, 2020; Plant *et al.*, 2021), we expected an overlap in binding targets between TPL and TPR1. Indeed, TPR1-GFP was enriched at several TPL targets found with ChIP-qPCR such as *Constans* (Goralogia *et al.*, 2017), *Apetala 3* (Gorham *et al.*, 2018), *Circadian clock associated 1*, *Leafy* and others (Lee *et al.*, 2020) in both *TPR1* Col or *TPR1 eds1* (Fig. S4). Hence, the TPR1-GFP ChIP-seq profiles in our study provide a genome-wide landscape to identify TPL/TPR targets of interest.

TPR1 shares binding targets with MYC2, SARD1 and WRKY TFs

The genome-wide profiles of TPR1-chromatin associations in immune-activated and non-activated leaf tissues prompted us to investigate if certain DNA motifs correlate with TPR1 binding. A *de novo* motif search revealed strong enrichment of the GAGA motif (C-box) under TPR1 peaks in *TPR1* Col and *TPR1 eds1* (Fig. S5a). The G-box (CACGTG) bound by MYC2 and other bHLH TFs was also over-represented under TPR1-GFP peaks in *TPR1 eds1* (Fig. S5a). We validated this signature by reanalyzing published MYC2 ChIP-seq profiles (Fig. 2f, S5b). A MYC2 ChIP signal (Wang *et al.*,

342   2019) was higher at promoters of genes bound by TPR1-GFP in both *TPR1* Col and

343   *TPR1 eds1* compared to their genome-wide level (Fig. 2f). TPR1-bound genes showed

344   statistically significant enrichment of MYC2 targets from two other studies ((Van

345   Moerkercke *et al.*, 2019; Zander *et al.*, 2020), Fig. S5b). Our *de novo* motif searches

346   did not find evidence for the enrichment of W-box 'TTGACY' bound by WRKYs

347   (Ciolkowski *et al.*, 2008) or the 'GAAATTT' element bound by SARD1 (Sun *et al.*,

348   2015). Considering the importance of these TFs in immune response regulation, we

349   specifically examined the distribution of WRKY and SARD1 TFs binding at TPR1-GFP

350   bound genes using available ChIP-seq data ((Sun *et al.*, 2015; Birkenbihl *et al.*, 2018),

351   (Fig. 2f, S5c,d). Both the metaplots and enrichment analyses for sets of genes

352   associated with TPR1 and TF peaks revealed that WRKY TFs and SARD1 binding

353   sites strongly overlap with those for TPR1-GFP relative to genome-wide levels (Fig. 2f,

354   S5c,d). These results suggest that TPR1 shares some *in vivo* binding targets with

355   MYC2, SARD1 and WRKY TFs.

356

357   **TPL/TPRs suppress prolonged expression of TNL[RRS1-RPS4] ETI-induced genes**

358   To explore functions of TPR1 and other TPL/TPRs in pathogen defense, we infiltrated

359   *Arabidopsis tpr1* and a *tpr1 tpl tpr4* triple (*t3*) mutant with virulent *Pst* (EV) or avirulent

360   (TNL[RRS1-RPS4]-inducing) *Pst avrRps4* bacteria alongside Col and hyper-susceptible Col

361   *eds1-2* (*eds1*). Growth of *Pst* and *Pst avrRps4* in the *tpr1* and *t3* mutants was not

362   different to Col at 3 d (Fig. 3a,b). *Arabidopsis* TPL represses MYC2 activity (Pauwels

363   *et al.*, 2010) which, when activated via bacterial coronatine, antagonizes *EDS1*- and

364   *ICS1*/SA-dependent bacterial resistance (Cui *et al.*, 2018; Bhandari *et al.*, 2019). We

365   therefore tested whether defects of *tpr1* and *t3* mutants in bacterial resistance are

366   masked by coronatine-promoted susceptibility. For this, we infiltrated *tpr1* and *t3* plants

367   with coronatine-deficient *Pst Δcor* or *Pst Δcor avrRps4* (Fig. 3c,d)*. A mutant of the

368   coronatine insensitive 1 (COI1) JA coreceptor was included as a negative control since

369   virulent *Pseudomonas* bacteria hijack COI1 to suppress SA-dependent defenses

370   (Zheng *et al.*, 2012). As expected, *Pst* coronatine-promoted virulence was

371   counteracted by avrRps4-activated TNL$^{RRS1-RPS4}$ ETI ((Cui *et al.*, 2018; Bhandari *et al.*,

372   2019); Fig. 3a,c) and Col displayed bacterial coronatine-dependent susceptibility

373   compared to *coi1* plants (Fig. 3b,d). However, differences in bacterial growth between

374   Col and *t3* mutant remained marginal (<1 $\log_{10}$; Fig. 3c,d). We concluded that

375   TPL/TPRs are not essential for restricting bacterial growth in *Arabidopsis* immunity.

376   Since TPR1-GFP binds genes that are induced during the *EDS1*-dependent immune

377   signaling (Fig. 2d,e) but bacterial resistance was not compromised in *tpr1* and *t3* (Fig.

378   3a,b), we hypothesized that TPL/TPRs repress activated defense gene expression in

379   the immune response. To test this, we performed RNA-seq on leaves of the *tpr1* and

380   *t3* mutants alongside Col and *eds1* infiltrated with *Pst avrRps4*. In TNL$^{RRS1-RPS4}$ ETI,

381   the timing of *EDS1*-dependent transcriptional reprograming for effective immunity

382   was previously determined as 4-8 hpi (Bhandari *et al.*, 2019; Saile *et al.*, 2020; Sun *et*

383   *al.*, 2021). Leaves of 5-6-week-old plants were infiltrated with *Pst avrRps4* and samples

384   collected at 0 (~5 min), 8 and 24 hpi (Table S10). As expected, the number of

385   transcriptionally induced genes was higher in Col compared to *eds1* at 8 (2,097 genes)

386   and 24 (1,289 genes) hpi (Table S10, $\log_2 FC \geq 1$, FDR$\leq$0.05). By contrast, no DEGs

387   were detected between Col and *tpr1* or *t3* mutants at these time points (Table S10,

388     $\log_2 FC \geq 1$, FDR$\leq$0.05). We concluded that TPL/TPRs are likely dispensable for the

389   transcriptional mobilization of defense in TNL$^{RRS1-RPS4}$ mediated ETI to *Pst* bacteria.

390   Within the set of 1,289 genes with higher expression in Col vs *eds1* at 24 hpi (Table

391   S10, $\log_2 FC \geq 1$, FDR$\leq$0.05), we identified, respectively, 282 and 363 genes with 1.5

392   times higher expression in *tpr1* and *t3* than in Col (not statistically significant in terms

393   of adjusted p-value) including *ICS1*, *PAD4* and *Pathogenesis-related* 1 (*PR1*). Only 33

394   and 28 genes had 1.5 times lower expression in *tpr1* and *t3* compared to Col at 24 hpi

395   (not statistically significant, adjusted p-value). We applied a gene set analysis to test

396   whether functionally coherent gene groups rather than individual genes are hyper-

397   expressed in *tpr1* and *t3* immune responses. GO-based gene sets differentially

398   expressed relative to Col in one of the mutant lines (*eds1*, *tpr1*, *t3*) at 0, 8 or 24 h are

399   shown in heatmaps (Fig. 3e, S6a) and Table S11 ($|\log_2 FC| \geq 0.5$, FDR$\leq$0.01). At 0 hpi

400   (~5 min after *Pst avrRps4* infiltration), *eds1*, *tpr1* and *t3* had reduced expression of

401   genes with GO terms "systemic acquired resistance" and "response to bacterium" (Fig.

402   3c, S6a,b), likely reflecting basal stress of leaf infiltration compared to no treatment

403   (Fig. S6c, (Bhandari *et al.*, 2019; Van Moerkercke *et al.*, 2019)). At 8 hpi, *tpr1* and *t3*

404   mutants were indistinguishable from Col (Fig. S6a,b), underscoring the dispensability

405   of TPL/TPRs for early transcriptional mobilization and pathogen resistance (Fig. 3a,

406   (Ding *et al.*, 2020)). Strikingly, at 24 hpi gene sets corresponding to GO terms "systemic

407   acquired resistance" and "response to bacterium" had elevated expression in *tpr1* and

408   *t3* mutants compared to Col (mean $\log_2 FC = 0.29$, FDR<0.05; Fig. 3e, S6a,b).

409   Furthermore, groups of genes that were co-targeted by TPR1 and SARD1, WRKY,

410   MYC2 TFs showed increased expression in the *t3* mutant at 24 hpi (mean

411     $\log_2 FC = 0.25$, 0.20, and 0.27, FDR<0.05; Fig. S7a,b; clusters of genes are given in

412   Table S12). These results suggest that TPL/TPRs mildly repress defense gene

413   expression after the initial wave of transcriptional elevation in a TNL[RRS1-RPS4] ETI

414   response.

415
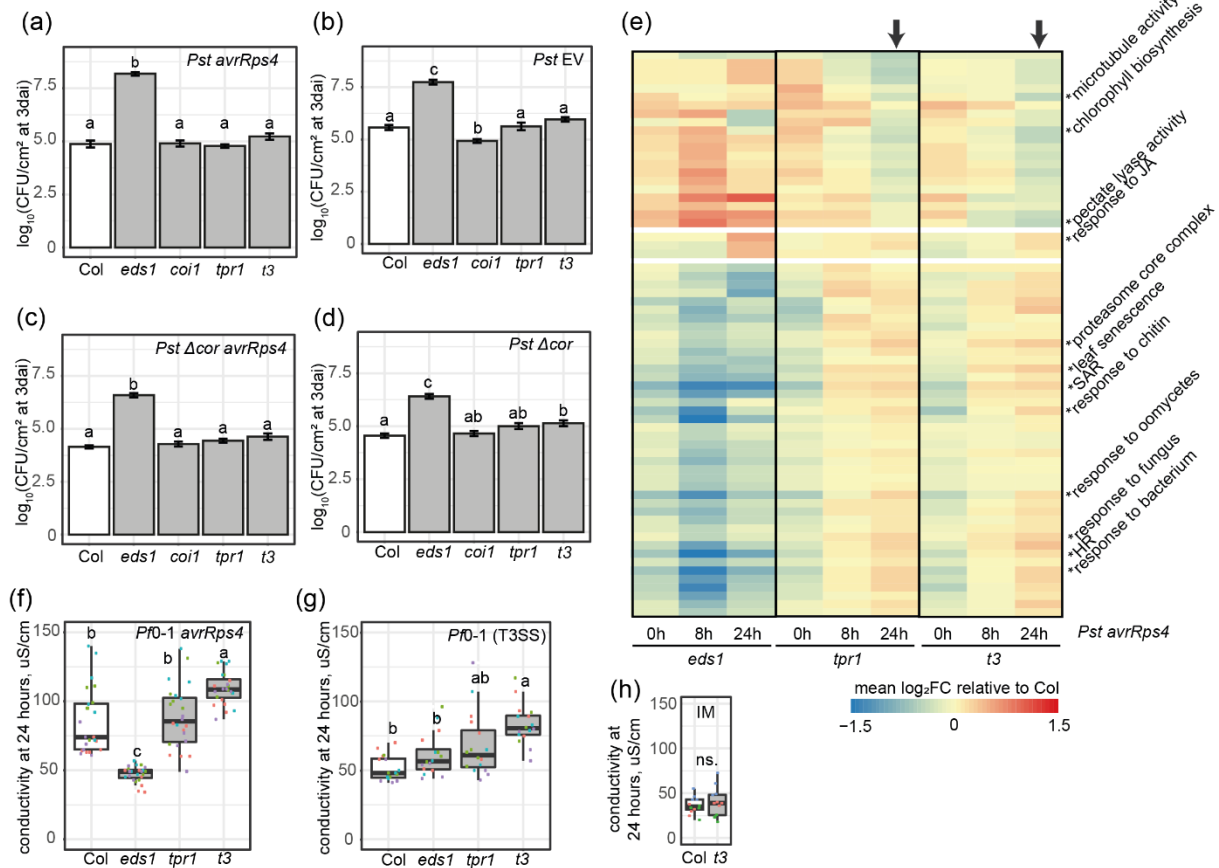
Fig. 3 Role of *Arabidopsis TPL/TPRs* in restricting of bacteria-triggered host defense-related transcriptional reprogramming and electrolyte leakage. (a-d) Titers of *Pseudomonas syringae pv. tomato* DC3000 (*Pst*) *avrRps4* (a), *Pst* (b), *Pst avrRps4 Δcor* (c) *Pst Δcor* (d) bacteria in indicated *Arabidopsis* mutants relative to Col plants. *eds1* mutant served as a susceptibility control, and the *coi1* mutant - as a readout for the coronatine promoted susceptibility. The *tpr1* and *tpr1 tpl tpr4* (*t3*) mutants showed Col-like levels of the *Pst avrRps4* and *Pst* growth (Tukey's HSD, α=0.001; n=22 from four independent experiments with *Pst avrRps4* and n=46 from eight independent experiments with *Pst*). **(e)** Heatmap of mean expression values for genes associated with selected GO terms in indicated mutants relative to Col after syringe-infiltration of *Pst avrRps4* (OD$_{600}$=0.001). Shown GO terms were differentially expressed in one of the genotypes relative to Col (|log$_2$FC|≥0.58 or 1.5 times, t-test FDR<0.05, asterisk show where the GO terms are on the heatmap). The *tpr1* and *t3* mutants displayed significant increase in the expression of genes from defense-related GO terms at 24 h (black arrow), e.g. "systemic acquired resistance" (SAR) and "response to bacterium". The "0 hour" time point refers to ~5 minutes after the infiltration. **(f, g)** Electrolyte leakage in *Arabidopsis* plants of indicated genotypes in response to non-virulent *Pseudomonas fluorescens* bacteria *Pf*0-1 equipped with type III secretion system (T3SS) and expressing (f) or not (g) the avrRps4 effector. The *t3* mutant displayed increased electrolyte leakage at 24 hpi with these strains (Tukey's HSD, α=0.001; n=16 from four independent experiments). **(h)** The differential electrolyte leakage response in *t3* is bacteria-triggered since the infiltration of 10 mM MgCl$_2$ (infiltration medium, IM) gave similar conductivity levels in Col-0 and *t3* at 24 h (ANOVA, p>0.05).

tpr1 tpl tpr4 mutants display enhanced PTI-linked electrolyte leakage

Next we tested whether TPL/TPRs help to restrict an extended immune response without compromising resistance (see Fig. 3a,b). In TNL$^{RRS1-RPS4}$ ETI, host cell death measured as electrolyte leakage can be uncoupled from bacterial growth restriction

19

422 (Heidrich *et al.*, 2011; Lapin *et al.*, 2019; Saile *et al.*, 2020). We therefore quantified

423 electrolyte leakage in the *tpr1* and *t3* mutants after infiltration of the type III secretion

424 system (T3SS) equipped effector-tester strain of *Pseudomonas fluorescens* (*Pf*) 0-1

425 strain delivering avrRps4. At 24 h after *Pf*0-1 *avrRps4* infiltration, conductivity was

426 higher in Col than *eds1*, consistent with *EDS1* being essential for TNL triggered cell

427 death ((Heidrich *et al.*, 2011; Lapin *et al.*, 2019; Saile *et al.*, 2020), Fig. 3f). While *tpr1*

428 plants behaved similarly to Col, the *t3* mutant had increased conductivity at 24 hpi

429 compared to Col (Fig. 3f). The same *Arabidopsis* lines were infiltrated with the tester

430 strain *Pf*0-1 that elicits PTI (Sohn *et al.*, 2014; Saile *et al.*, 2020). T3SS-equipped *Pf*0-

431 1 also led to increased electrolyte leakage in the *t3* mutant at 24 hpi compared to Col

432 plants (Fig. 3g). No differences in electrolyte leakage were found between Col and *t3*

433 under mock conditions (Fig. 3h). These observations show that the *tpr1 tpl tpr4* mutant

434 is defective in limiting bacteria-triggered immunity signaling. We therefore propose that

435 one potentially important and hitherto unknown role of TPL/TPRs is to prevent an over-

436 reaction of host tissues to pathogen infection.

437

438 **TPR1 limits *ICS1* and *MYC* TF-promoted PTI electrolyte leakage**

439 We generated three independent stable homozygous complementation lines

440 expressing *pTPR1:TPR1-GFP* in the *t3* background. None of these displayed the

441 *TPR1* Col-like growth retardation or high TPR1-GFP protein accumulation (Fig. 4a,b).

442 The enhanced electrolyte leakage in *t3* after *Pf*0-1 EV infiltration was reduced to Col

443 levels in the three transgenic lines expressing different levels of TPR1-GFP protein

444 (Fig. 4b,c), suggesting a role of TPR1 in limiting PTI[*Pf*0-1 (T3SS)]-related electrolyte

445 leakage.

446 TPR1-GFP associated with the promoters of *ICS1* (Fig. S2) and MYC2-bound genes

447 in the *TPR1* Col ChIP-seq analysis (Fig. 2f, S5b). Since SA and JA signaling contribute

20

448   to PTI (Tsuda *et al.*, 2009; Mine *et al.*, 2017), we assessed whether a *sid2/ics1* mutant*,*

449   a *myc2 myc3 myc4* (*myc234*) triple mutant, or a combined *myc234 sid2* quadruple

450   mutant show altered PTI-related electrolyte leakage. We found that the electrolyte

451   leakage triggered by the *Pf*0-1 tester strain at 24 h was reduced in the *myc234 sid2*

452   mutant compared to Col. Taken together, our data show that TPR1 dampens *ICS1-*

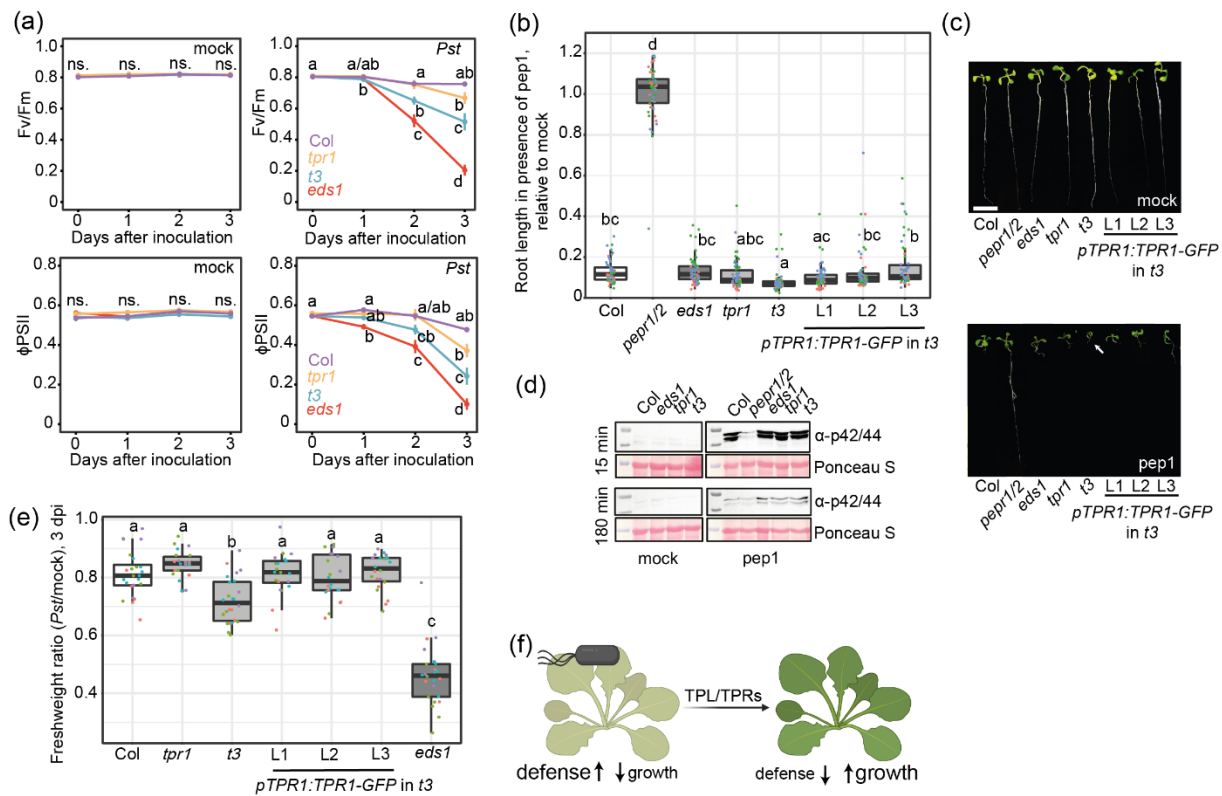453   and *MYC2,3,4*-dependent immune responses after their activation by bacteria.
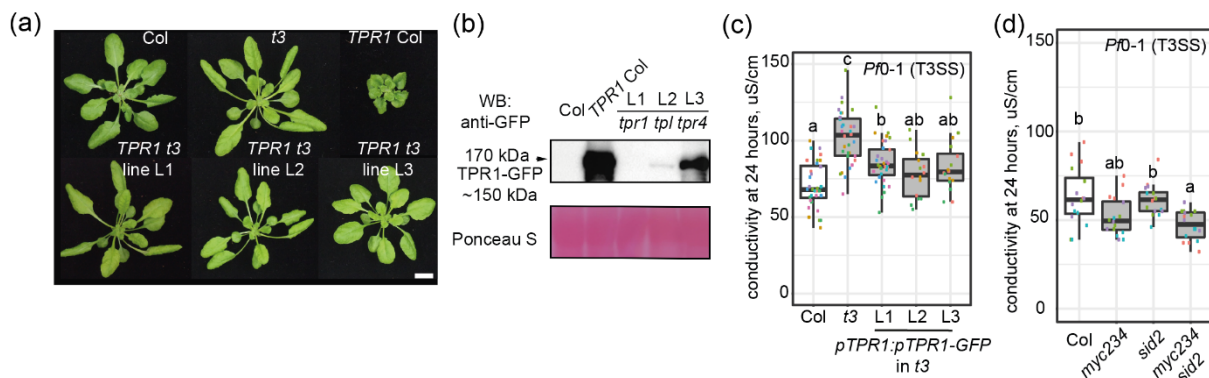
454

Fig. 4 *Arabidopsis* TPR1 counteracts electrolyte leakage triggered by the T3SS-equipped *Pf*0-1 bacteria and promoted by *ICS1* and *MYC* TFs. (a) Representative photos of rosettes of 5-6-week-old plants from three independent T3 homozygous complementation lines expressing *pTPR1:TPR1-GFP* in *tpr1 tpl tpr4* (*t3*). *TPR1* Col is shown for comparison. The complementation lines do not show dwarfism in contrast to *TPR1* Col with the constitutive defense signaling. **(b)** Steady-state levels of TPR1-GFP in lines from (a), determined via Western blot analysis. Total protein extracts were probed with α-GFP antibodies. Ponceau S staining was used to control loading. The experiment was repeated two times with similar results. **(c)** Electrolyte leakage in the complementation lines from (a) and control lines Col and *t3* at 24 h after the *Pf*0-1 T3SS (OD$_{600}$=0.2) infiltration. The complementation lines L1-L3 show a level of the electrolyte leakage comparable to Col (Tukey's HSD α=0.001; different colors of data points correspond to independent experiments, n=12-24 from three or six independent experiments). **(d)** Electrolyte leakage in leaf discs of indicated genotypes after the *Pf*0-1 T3SS infiltration (Tukey's HSD α=0.001; different colors of data points correspond to independent experiments, n=16 from four independent experiments). The high order mutant *myc2 myc3 myc4 sid2* (*myc234 sid2*) shows lower conductivity than Col.

455

21

456   **TPL/TPRs reduce physiological damage associated with prolonged immunity**

457   Because *Arabidopsis* TPR1 and TPL/TPRs appear to globally limit the expression of

458   induced defense-related genes (Fig. 3e, S6a,b, S7a,b) without compromising bacterial

459   resistance (Fig. 3a,b), we speculated that these transcriptional corepressors reduce

460   adverse effects of bacteria-activated defenses on plant growth and physiology. We

461   tested whether TPL/TPRs help to maintain photosynthetic efficiency in infected plants

462   by quantifying photosystem II (PSII) fluorescence. While alterations of the operating

463   PSII efficiency (ϕPSII) are measurable during short-term stress, a drop in the maximum

464   quantum yield of PSII (F_v/F_m) reflects more acute damage to PSII, and is observed

465   under prolonged stress conditions (Baker, 2008). The *tpr1* and *t3* mutants were

466   infiltrated alongside Col with a low dose of *Pst* bacteria (OD_{600}=0.005). A reduction in

467   ϕPSII and F_v/F_m values was minimal in infected Col leaves over the course of 3 d,

468   indicating that these plants effectively balance bacterial growth restriction and PSII

469   performance (Figure 5A, purple line). By contrast, *tpr1* and more obviously *t3* mutant

470   lines, showed a decrease in ϕPSII and F_v/F_m over 3 d relative to Col (Fig. 5a; orange

471   line – *tpr1*, blue line – *t3*), despite having similar total chlorophyll as Col at 3 d after

472   infection (Fig. S8a). We concluded that a likely role of TPL/TPRs is to reduce collateral

473   damage of activated host defenses and thus maintain crucial photosynthetic functions.

474

22

Fig. 5 Role of TPL/TPRs in limiting adverse effects of activated immune system on *Arabidopsis* physiology and growth. (a) Maximum quantum yield of PSII (F_v/F_m) (upper panels) and operating PSII efficiency (ϕPSII) (lower panels) in indicated genotypes over the three-day time course after syringe infiltration of *Pst* (OD_{600}=0.005; left panels). Compared to Col, the *t3* mutant shows significantly reduced F_v/F_m at 3 days after infection with *Pst* but not in the mock-treated samples (Tukey's HSD α=0.05; n=9-12 from three independent experiments). **(b)** Boxplot representation of root growth inhibition caused by pep1 (200 nM) in 10-day-old seedlings of indicated genotypes grown on 0.5x liquid MS medium (Tukey's HSD α=0.05; n=58 from three independent experiments). **(c)** Representative photos of seedlings from (b). The *t3* is overly sensitive to pep1 at the level of root growth, and this phenotype is complemented in three independent complementation lines *pTPR1:TPR1-GFP* (in *t3* background). Scale bar = 1 cm **(d)** MPK3 and MPK6 phosphorylation assessed via Western blot analysis with α-p42/44 antibodies in indicated genotypes at 15 and 180 min after mock (mQ water) or pep1 (200 nM) treatment. The *t3* mutant showed Col level of MPK3 and MPK6 phosphorylation. (b-d) *eds1-12* was used as *eds1*. The experiment was repeated three times with similar results. **(e)** Fresh weight reduction in leaves inoculated with *Pst* (OD_{600}=0.005) compared to mock-treated leaves in indicated genotypes 3 days after infiltration (Tukey's HSD α=0.05; n=20-24 from four independent experiments). **(f)** Model of the function of TPR1 and other TPL/TPRs in immune-triggered Arabidopsis leaves. TPL/TPRs are not essential for limiting bacterial growth but help the plant to maintain PSII activity and growth after the activation of immune responses. The picture was created with BioRender.com.

475

476

23

477 Our model of TPL/TPRs limiting adverse effects of activated immunity on plant

478 physiology predicts that the *t3* mutant would be overly sensitive to an exposure to

479 bacterial PAMP such as flg22 or the phytocytokine pep1 at the level of root growth.

480 While primary root growth inhibition (RGI) was similar in Col, *tpr1* and *t3* mutants in the

481 presence of flg22 (Fig. S8b,c), RGI on the pep1-supplemented medium was more

482 pronounced in the *t3* mutant (Fig. 5b,c). Hyper-sensitivity of *t3* seedlings to pep1 was

483 rescued in the *TPR1-GFP* complementation lines (Fig. 5b,c). Perception of pep1 was

484 not altered in *t3* because pep1-induced mitogen-activated protein kinase 3 and 6

485 (MPK3 and MPK6) phosphorylation was similar to Col (Fig. 5d). Hence, TPR1 and

486 other TPL/TPRs reduce negative effects of activated immunity on root growth in

487 phytocytokine-stimulated sterile seedlings. Finally, we tested whether *Arabidopsis*

488 TPL/TPRs limit a host growth penalty in response to bacterial infection. We infiltrated

489 leaves of 5-6-week-old Col, *tpr1*, *t3* and *TPR1* complementation lines (in the *t3*

490 background) with 10 mM $MgCl_2$ (mock) or virulent *Pst* bacteria (OD_{600}=0.005) and

491 measured fresh weight of extracted leaf discs at 3 dpi. Whereas *Pst*-infected Col leaves

492 lost ~20% fresh weight, *t3* mutant leaves lost ~30%, which was recovered to Col levels

493 in the *TPR1-GFP* complementation lines (Fig. 5e). Taken together, the data suggest

494 that *Arabidopsis* TPR1 and other TPL/TPRs limit physiological and growth penalties

495 associated with induced immunity to bacteria.

496

497 **Discussion**

498 Timely activation and control of immune responses is essential for plant resilience to

499 pathogens. How activated defenses are restricted to prevent damaging over-reaction

500 of tissues is less clear. Here we present evidence that the TPL family of transcriptional

501 corepressors contribute to limiting physiological damage and growth inhibition

502   associated with host induced immunity, and therefore might be important components

503   for maintaining plant vital functions and productivity under pathogen stress.

504   We present ChIP-seq chromatin binding profiles for *Arabidopsis* TPR1 with or without

505   constitutive *EDS1*-dependent defense. TPR1-GFP associated with immediate

506   upstream regions of ~1,400 genes and ~10% of these genes showed enhanced TPR1-

507   GFP binding when *EDS1*-dependent immunity signaling was active (Fig. 2). Our data

508   suggest that TPR1 and other TPL/TPRs limit the expression of defense-promoted

509   genes after their initial activation during bacterial infection (Fig. 3). We further discover

510   a role of TPL/TPRs in reducing the damage to photosystem II and weight loss in

511   bacteria-infected leaves or seedling growth inhibition elicited by the pep1

512   phytocytokine (Fig. 5). Hence, we propose that *Arabidopsis* TPR1 and other TPL/TPRs

513   transcriptional corepressors mitigate adverse effects of activated immunity signaling

514   on host physiology and growth (Fig. 5f).

515   TPR1-GFP associated primarily with genic regions immediately upstream of the

516   transcription start site (TSS). This ChIP pattern is consistent with a role of TPL/TPRs

517   in physical interaction with DNA-binding TFs (Szemenyei *et al.*, 2008; Causier *et al.*,

518   2012) and with the location of predicted TF binding sites being predominantly close to

519   the TSS (Yu *et al.*, 2016). The TPR1-bound genes we detected are strongly enriched

520   for ChIP signals of MYC2 (Van Moerkercke *et al.*, 2019; Wang *et al.*, 2019; Zander *et*

521   *al.*, 2020), WRKYs (Birkenbihl *et al.*, 2018), and SARD1 (Sun *et al.*, 2015) TFs (Fig.

522   2f). Whether TPR1 forms complexes with MYC, WRKY and SARD1 TFs *in planta*

523   during pathogen infection remains unclear.

524   In addition to immunity-related functions, TPR1-GFP bound genes are enriched for GO

525   terms associated with control of growth and development (Tables S6, S7). More

526   specifically, the *TPR1 eds1* ChIP-seq profile might be informative for studies of

527   TPL/TPR-chromatin interactions in growth and development (Fig. S4; (Goralogia *et al.*,

25

528   2017; Gorham *et al.*, 2018; Lee *et al.*, 2020; Plant *et al.*, 2021)) since autoimmunity

529   effects are lost in this line (Fig. 1). We provide processed input-normalized TPR1-GFP

530   enrichment profiles for both *TPR1* Col and *TPR1 eds1* at nucleotide resolution and

531   scripts to prepare metaplots for the genes of interest in R environment (see Methods

532   S1 and Data availability section).

533   TPR1 was proposed to promote defense by repressing negative regulators of

534   resistance (Zhu *et al.*, 2010). Consistent with this view, TPR1 is enriched at promoters

535   of genes that are repressed during TNL$^{RRS1-RPS4}$ ETI (Bartsch *et al.*, 2006; Zhu *et al.*,

536   2010) and can repress *DND1/CNGC2* and *DND2/CNGC4* promoter activity (Niu *et al.*,

537   2019). This idea is further supported by the observations that MYC2, which interacts

538   with and is repressed by TPL complexes (Pauwels *et al.*, 2010), antagonizes *EDS1-*

539   dependent bacterial resistance (Cui *et al.*, 2018; Bhandari *et al.*, 2019). Based on our

540   data, we present here a more refined picture of TPR1 functions. In the extended model,

541   TPR1 binds genes induced early during a bacterial infection and prevents their

542   prolonged over-expression (Fig. 5f). In support of this, ~ 10% of TPR1 binding was

543   contingent on *EDS1*-mediated immunity (Fig. 2). These targets included *ICS1* (Fig. S2)

544   which is important for resistance to a range of biotrophic and hemi-biotrophic

545   pathogens (Ding & Ding, 2020). Second, the *t3* mutant showed elevated expression of

546   gene sets co-targeted by TPR1-GFP and MYC2, SARD1, and WRKY TFs (Fig. 3e) at

547   24 h after infection with *Pst avrRps4*. Third, *ICS1/MYCs*-dependent PTI-elicited

548   electrolyte leakage was enhanced in *t3* mutants (Fig. 3g) but recovered in

549   complementation *TPR1-GFP* lines (Fig. 4). The enhanced defense responses of *t3*

550   resemble hypersensitivity of *tpl* to MeJA at the level of root growth (Pauwels *et al.*,

551   2010).

552   Several studies have suggested a positive role of TPR1 in the regulation of TNL and

553   basal immunity signaling (Zhu *et al.*, 2010; Zhang *et al.*, 2019; Harvey *et al.*, 2020;

554   Navarrete *et al.*, 2021). Indeed, we observed mildly delayed expression of genes from

555   immunity-linked GO terms in *tpr1* and *t3* within minutes of *Pst avrRps4* infiltration (Fig.

556   4A). This might be attributed to the reduced PAMP flg22-triggered ROS burst in *tpl* and

557   *t3* mutants (Navarrete *et al.*, 2021). Although immediate early responses contributing

558   to PTI involve CAMTA TFs (Jacob *et al.*, 2018; Bjornson *et al.*, 2021), no enrichment

559   of CAMTA-bound DNA motifs was found under TPR1 peaks in our ChIP-seq

560   experiments (Fig. S5). We also detected marginally increased susceptibility of the *t3*

561   mutant to *Pst ⊿cor* bacteria impaired in the ability to manipulate host MYC2/JA

562   signaling (Fig. 3d). The removal of different sectors of immunity signaling in the *t3*

563   mutant might facilitate analysis of the TPR1 positive role in NLR and basal resistance.

564   Timely downregulation of defense signaling is relevant because prolonged pathogen

565   infection and plant immune activation often lead to reduced photosynthetic activity and

566   biomass accumulation regardless of the plant's ability to cope with the stress of

567   infections and disease (Walters, 2015a; Walters, 2015b). Accordingly, pathogen-free

568   induction of SA and JA signaling is associated with reduced expression of genes

569   involved in photosynthesis (Hickman *et al.*, 2017; Hickman *et al.*, 2019). Despite

570   identification of multiple genes impacting the balance between plant growth and

571   defense (Huot *et al.*, 2014; Bruessow *et al.*, 2021), knowledge of how infected plants

572   turn off transcriptional defenses and regain physiological homeostasis is fragmentary.

573   Cytoplasmic condensates of the SA receptor NPR1 were reported to be responsible

574   for the ubiquitination of ETI cell death-promoting WRKY TFs to limit their activities

575   (Zavaliev *et al.*, 2020). Also, an SA receptor, NPR4, suppresses *Arabidopsis* WRKY70

576   promoter activity (Ding *et al.*, 2018). We find that the *tpr1* and *t3* mutants are defective

577   in maintaining optimal photosystem II function, even though resistance to *Pst* bacteria

578   was largely intact in these mutants (Fig. 3b, 5a). Similarly, loss of fresh weight in *Pst-*

27

579 infected *t3* was more extreme than in Col or the *TPR1* complementation lines (Fig. 5e),

580 and *t3* seedlings treated with the phytocytokine pep1-triggered RGI was stronger in *t3*

581 than Col plants (Fig. 5b,c). Hence, our study identifies the *Arabidopsis* transcriptional

582 corepressor TPR1 as a factor that prevents overshooting of an immune response and

583 therefore potentially as a contributor to plant stress-fitness balance.

584

Acknowledgements

594

Author Contribution

596 TG, DL, FL, JEP designed the experiments; TG, DL, FL performed the experiments;
597 TG, DL, JEP analyzed all data; BK, LC, MB analyzed ChIP-seq and RNA-seq; JB, DL
598 generated and characterized complementation lines; JQ generated *myc234sid2* line;
599 DL prepared the Github repository and materials to access processed ChIP-seq data;
600 TG, DL and JEP wrote the manuscript with input from all authors.

601

Data availability

603 RNA-seq and ChIP-seq data from this article are deposited in the National Center for
604 Biotechnology Information Gene Expression Omnibus (GEO) database with
605 accession numbers GSE149316, GSE154652, GSE154774. Bigwig, BAM and BAI
606 files of TPR1 ChIP-seq for visualization in IGV browser are also available through the
607 Max Planck Digital Library collection (MPDL;
608 https://edmond.mpdl.mpg.de/imeji/collection/U6N5zIOIWgjjMZCu). Scripts for
609 preparing metaplots in R environment on a personal computer (~8G RAM) are on
610 GitHub (https://github.com/rittersporn/TPR1_metaplots_Griebel_Lapin_etal_2021).
611

References

Albert I, Hua C, Nürnberger T, Pruitt RN, Zhang L. 2020. Surface Sensor Systems in Plant Immunity. *Plant Physiology* **182**(4): 1582-1582.

Ariga H, Katori T, Tsuchimatsu T, Hirase T, Tajima Y, Parker JE, Alcázar R, Koornneef M, Hoekenga O, Lipka AE, et al. 2017. NLR locus-mediated trade-off between abiotic and biotic stress adaptation in Arabidopsis. *Nature Plants* **3**(6): 17072.

Baker NR. 2008. Chlorophyll Fluorescence: A Probe of Photosynthesis In Vivo. *Annual Review of Plant Biology* **59**(1): 89-113.

Bartsch M, Gobbato E, Bednarek P, Debey S, Schultze JL, Bautor J, Parker JE. 2006. Salicylic acid-independent ENHANCED DISEASE SUSCEPTIBILITY1 signaling in Arabidopsis immunity and cell death is regulated by the monooxygenase FMO1 and the Nudix hydrolase NUDT7. *The Plant Cell* **18**(4): 1038-1051.

Bhandari DD, Lapin D, Kracher B, von Born P, Bautor J, Niefind K, Parker JE. 2019. An EDS1 heterodimer signalling surface enforces timely reprogramming of immunity genes in Arabidopsis. *Nature Communications* **10**(1): 772.

Birkenbihl RP, Kracher B, Roccaro M, Somssich IE. 2017. Induced Genome-Wide Binding of Three Arabidopsis WRKY Transcription Factors during Early MAMP-Triggered Immunity. *The Plant Cell* **29**(1): 20-38.

Birkenbihl RP, Kracher B, Ross A, Kramer K, Finkemeier I, Somssich IE. 2018. Principles and characteristics of the Arabidopsis WRKY regulatory network during early MAMP-triggered immunity. *The Plant Journal* **96**(3): 487-502.

Bjornson M, Pimprikar P, Nürnberger T, Zipfel C. 2021. The transcriptional landscape of Arabidopsis thaliana pattern-triggered immunity. *Nature Plants* **7**(5): 579-586.

Bruessow F, Bautor J, Hoffmann G, Yildiz I, Zeier J, Parker JE. 2021. Natural variation in temperature-modulated immunity uncovers transcription factor bHLH059 as a thermoresponsive regulator in Arabidopsis thaliana. *PLOS Genetics* **17**(1): e1009290.

Caarls L, Elberse J, Awwanah M, Ludwig NR, de Vries M, Zeilmaker T, Van Wees SCM, Schuurink RC, Van den Ackerveken G. 2017. Arabidopsis JASMONATE-INDUCED OXYGENASES down-regulate plant immunity by hydroxylation and inactivation of the hormone jasmonic acid. *Proceedings of the National Academy of Sciences* **114**(24): 6388-6393.

Causier B, Ashworth M, Guo W, Davies B. 2012. The TOPLESS Interactome: A Framework for Gene Repression in Arabidopsis. *Plant Physiology* **158**(1): 423-438.

Ciolkowski I, Wanke D, Birkenbihl RP, Somssich IE. 2008. Studies on DNA-binding selectivity of WRKY transcription factors lend structural clues into WRKY-domain function. *Plant Molecular Biology* **68**(1): 81-92.

Clough SJ, Fengler KA, Yu I-c, Lippok B, Smith RK, Bent AF. 2000. The Arabidopsis dnd1 "defense, no death" gene encodes a mutated cyclic nucleotide-gated ion channel. *Proceedings of the National Academy of Sciences* **97**(16): 9323-9328.

Cui H, Qiu J, Zhou Y, Bhandari DD, Zhao C, Bautor J, Parker JE. 2018. Antagonism of Transcription Factor MYC2 by EDS1/PAD4 Complexes Bolsters Salicylic Acid Defense in Arabidopsis Effector-Triggered Immunity. *Molecular Plant* **11**(8): 1053-1066.

Cui H, Tsuda K, Parker JE. 2015. Effector-Triggered Immunity: From Pathogen Perception to Robust Defense. *Annual Review of Plant Biology* **66**(1): 487-511.

Darino M, Chia K-S, Marques J, Aleksza D, Soto-Jiménez LM, Saado I, Uhse S, Borg M, Betz R, Bindics J, et al. 2021. Ustilago maydis effector Jsi1 interacts with Topless corepressor, hijacking plant jasmonate/ethylene signaling. *New Phytologist* **229**(6): 3393-3407.

Deng Y, Zhai K, Xie Z, Yang D, Zhu X, Liu J, Wang X, Qin P, Yang Y, Zhang G, et al. 2017. Epigenetic regulation of antagonistic receptors confers rice blast resistance with yield balance. *Science* **355**(6328): 962-965.

Ding P, Ding Y. 2020. Stories of Salicylic Acid: A Plant Defense Hormone. *Trends Plant Sci* **25**(6): 549-565.

Ding P, Ngou BPM, Furzer OJ, Sakai T, Shrestha RK, MacLean D, Jones JDG. 2020. High-resolution expression profiling of selected gene sets during plant immune activation. *Plant Biotechnology Journal* **18**(7): 1610-1619.

Ding Y, Sun T, Ao K, Peng Y, Zhang Y, Li X, Zhang Y. 2018. Opposite Roles of Salicylic Acid Receptors NPR1 and NPR3/NPR4 in Transcriptional Regulation of Plant Immunity. *Cell* **173**(6): 1454-1467.

Dongus JA, Parker JE. 2021. EDS1 signalling: At the nexus of intracellular and surface receptor immunity. *Current Opinion in Plant Biology* **62**: 102039.

Dowen RH, Pelizzola M, Schmitz RJ, Lister R, Dowen JM, Nery JR, Dixon JE, Ecker JR. 2012. Widespread dynamic DNA methylation in response to biotic stress. *Proceedings of the National Academy of Sciences* **109**(32): E2183-2191.

Dvořák Tomaštíková E, Hafrén A, Trejo-Arellano MS, Rasmussen SR, Sato H, Santos-González J, Köhler C, Hennig L, Hofius D. 2021. Polycomb Repressive Complex 2 and KRYPTONITE regulate pathogen-induced programmed cell death in Arabidopsis. *Plant Physiology* **185**(4): 2003-2021.

Fernández-Calvo P, Chini A, Fernández-Barbero G, Chico J-M, Gimenez-Ibanez S, Geerinck J, Eeckhout D, Schweizer F, Godoy M, Franco-Zorrilla JM, et al. 2011. The Arabidopsis bHLH transcription factors MYC3 and MYC4 are targets of JAZ repressors and act additively with MYC2 in the activation of jasmonate responses. *The Plant Cell* **23**(2): 701-715.

679 **Fradin EF, Abd-El-Haliem A, Masini L, van den Berg GC, Joosten MH, Thomma BP. 2011.** Interfamily
680   transfer of tomato Ve1 mediates Verticillium resistance in Arabidopsis. *Plant Physiol* **156**(4): 2255-2265.
681 **Garner CM, Spears BJ, Su J, Cseke LJ, Smith SN, Rogan CJ, Gassmann W. 2021.** Opposing functions of the
682   plant TOPLESS gene family during SNC1-mediated autoimmunity. *PLOS Genetics* **17**(2): e1009026.
683 **Goralogia GS, Liu T-K, Zhao L, Panipinto PM, Groover ED, Bains YS, Imaizumi T. 2017.** CYCLING DOF
684   FACTOR 1 represses transcription through the TOPLESS co-repressor to control photoperiodic
685   flowering in Arabidopsis. *The Plant Journal* **92**(2): 244-262.
686 **Gorham SR, Weiner AI, Yamadi M, Krogan NT. 2018.** HISTONE DEACETYLASE 19 and the flowering time
687   gene FD maintain reproductive meristem identity in an age-dependent manner. *Journal of experimental*
688   *botany* **69**(20): 4757-4771.
689 **Harvey S, Kumari P, Lapin D, Griebel T, Hickman R, Guo W, Zhang R, Parker JE, Beynon J, Denby K, et al.**
690   **2020.** Downy Mildew effector HaRxL21 interacts with the transcriptional repressor TOPLESS to promote
691   pathogen susceptibility. *PLOS Pathogens* **16**(8): e1008835.
692 **Heidrich K, Wirthmueller L, Tasset C, Pouzet C, Deslandes L, Parker JE. 2011.** *Arabidopsis* EDS1 Connects
693   Pathogen Effector Recognition to Cell Compartment–Specific Immune Responses. *Science* **334**(6061):
694   1401-1404.
695 **Hickman R, Mendes MP, Van Verk MC, Van Dijken AJH, Di Sora J, Denby K, Pieterse CMJ, Van Wees SCM.**
696   **2019.** Transcriptional Dynamics of the Salicylic Acid Response and its Interplay with the Jasmonic Acid
697   Pathway. *bioRxiv*: 742742.
698 **Hickman R, Van Verk MC, Van Dijken AJH, Mendes MP, Vroegop-Vos IA, Caarls L, Steenbergen M, Van der**
699   **Nagel I, Wesselink GJ, Jironkin A, et al. 2017.** Architecture and Dynamics of the Jasmonic Acid Gene
700   Regulatory Network. *The Plant Cell* **29**(9): 2086-2105.
701 **Huang C-Y, Rangel DS, Qin X, Bui C, Li R, Jia Z, Cui X, Jin H. 2021.** The chromatin-remodeling protein
702   BAF60/SWP73A regulates the plant immune receptor NLRs. *Cell Host & Microbe* **29**(3): 425-434.e424.
703 **Huot B, Yao J, Montgomery BL, He SY. 2014.** Growth–Defense Tradeoffs in Plants: A Balancing Act to
704   Optimize Fitness. *Molecular Plant* **7**(8): 1267-1287.
705 **Igarashi D, Tsuda K, Katagiri F. 2012.** The peptide growth factor, phytosulfokine, attenuates pattern-triggered
706   immunity. *The Plant Journal* **71**(2): 194-204.
707 **Jacob F, Kracher B, Mine A, Seyfferth C, Blanvillain-Baufumé S, Parker JE, Tsuda K, Schulze-Lefert P,**
708   **Maekawa T. 2018.** A dominant-interfering camta3 mutation compromises primary transcriptional outputs
709   mediated by both cell surface and intracellular immune receptors in Arabidopsis thaliana. *New Phytol*
710   **217**(4): 1667-1680.
711 **Jones JDG, Vance RE, Dangl JL. 2016.** Intracellular innate immune surveillance devices in plants and animals.
712   *Science* **354**(6316): aaf6395.
713 **Jurkowski GI, Smith RK, Yu Ic, Ham JH, Sharma SB, Klessig DF, Fengler KA, Bent AF. 2004.** Arabidopsis
714   DND2, a Second Cyclic Nucleotide-Gated Ion Channel Gene for Which Mutation Causes the "Defense,
715   No Death" Phenotype. *Molecular Plant-Microbe Interactions®* **17**(5): 511-520.
716 **Ke J, Ma H, Gu X, Thelen A, Brunzelle JS, Li J, Xu HE, Melcher K. 2015.** Structural basis for recognition of
717   diverse transcriptional repressors by the TOPLESS family of corepressors. *Science Advances* **1**(6):
718   e1500107.
719 **Kuhn A, Ramans Harborough S, McLaughlin HM, Natarajan B, Verstraeten I, Friml J, Kepinski S,**
720   **Østergaard L. 2020.** Direct ETTIN-auxin interaction controls chromatin states in gynoecium
721   development. *eLife* **9**: e51787.
722 **Lapin D, Bhandari DD, Parker JE. 2020.** Origins and Immunity Networking Functions of EDS1 Family Proteins.
723   *Annual Review of Phytopathology* **58**(1): 253-276.
724 **Lapin D, Kovacova V, Sun X, Dongus JA, Bhandari D, von Born P, Bautor J, Guarneri N, Rzemieniewski J,**
725   **Stuttmann J, et al. 2019.** A Coevolved EDS1-SAG101-NRG1 Module Mediates Cell Death Signaling by
726   TIR-Domain Immune Receptors. *The Plant Cell* **31**(10): 2430-2455.
727 **Lee HG, Won JH, Choi Y-R, Lee K, Seo PJ. 2020.** Brassinosteroids Regulate Circadian Oscillation via the
728   BES1/TPL-CCA1/LHY Module in Arabidopsisthaliana. *iScience* **23**(9): 101528.
729 **Leng X, Thomas Q, Rasmussen SH, Marquardt S. 2020.** A G(enomic)P(ositioning)S(ystem) for Plant RNAPII
730   Transcription. *Trends in Plant Science* **25**(8): 744-764.
731 **Leydon AR, Wang W, Gala HP, Gilmour S, Juarez-Solis S, Zahler ML, Zemke JE, Zheng N, Nemhauser JL.**
732   **2021.** Repression by the Arabidopsis TOPLESS corepressor requires association with the core mediator
733   complex. *eLife* **10**: e66739.
734 **Liu L, Sonbol F-M, Huot B, Gu Y, Withers J, Mwimba M, Yao J, He SY, Dong X. 2016.** Salicylic acid receptors
735   activate jasmonic acid signalling through a non-canonical pathway to promote effector-triggered
736   immunity. *Nature Communications* **7**(1): 13099.
737 **Long JA, Ohno C, Smith ZR, Meyerowitz EM. 2006.** TOPLESS Regulates Apical Embryonic Fate in
738   *Arabidopsis*. *Science* **312**(5779): 1520-1523.
739 **Lorenzo O, Chico JM, Sánchez-Serrano JJ, Solano R. 2004.** JASMONATE-INSENSITIVE1 Encodes a MYC
740   Transcription Factor Essential to Discriminate between Different Jasmonate-Regulated Defense
741   Responses in Arabidopsis. *The Plant Cell* **16**(7): 1938-1950.
742 **Ma H, Duan J, Ke J, He Y, Gu X, Xu T-H, Yu H, Wang Y, Brunzelle JS, Jiang Y, et al. 2017.** A D53 repression
743   motif induces oligomerization of TOPLESS corepressors and promotes assembly of a corepressor-
744   nucleosome complex. *Science Advances* **3**(6): e1601217.
745 **Martin-Arevalillo R, Nanao MH, Larrieu A, Vinos-Poyo T, Mast D, Galvan-Ampudia C, Brunoud G, Vernoux**
746   **T, Dumas R, Parcy F. 2017.** Structure of the *Arabidopsis* TOPLESS corepressor provides insight into

747 the evolution of transcriptional repression. *Proceedings of the National Academy of Sciences* **114**(30): 8107.

749 **Mine A, Nobori T, Salazar-Rondon MC, Winkelmüller TM, Anver S, Becker D, Tsuda K. 2017.** An incoherent feed-forward loop mediates robustness and tunability in a plant immune network. *EMBO reports* **18**(3): 464-476.

752 **Mine A, Seyfferth C, Kracher B, Berens ML, Becker D, Tsuda K. 2018.** The Defense Phytohormone Signaling Network Enables Rapid, High-Amplitude Transcriptional Reprogramming during Effector-Triggered Immunity. *The Plant Cell* **30**(6): 1199-1219.

755 **Navarrete F, Gallei M, Kornienko AE, Saado I, Chia K-S, Darino MA, Khan M, Bindics J, Djamei A. 2021.** TOPLESS promotes plant immunity by repressing auxin signaling and is targeted by the fungal effector Naked1. *bioRxiv*: 2021.2005.2004.442566.

758 **Ngou BPM, Ahn H-K, Ding P, Jones JDG. 2021.** Mutual potentiation of plant immunity by cell-surface and intracellular receptors. *Nature* **592**(7852): 110-115.

760 **Niu D, Lin X-L, Kong X, Qu G-P, Cai B, Lee J, Jin JB. 2019.** SIZ1-Mediated SUMOylation of TPR1 Suppresses Plant Immunity in Arabidopsis. *Molecular Plant* **12**(2): 215-228.

762 **Ordon J, Gantner J, Kemna J, Schwalgun L, Reschke M, Streubel J, Boch J, Stuttmann J. 2017.** Generation of chromosomal deletions in dicotyledonous plants employing a user-friendly genome editing toolkit. *Plant J* **89**(1): 155-168.

765 **Pauwels L, Barbero GF, Geerinck J, Tilleman S, Grunewald W, Pérez AC, Chico JM, Bossche RV, Sewell J, Gil E, et al. 2010.** NINJA connects the co-repressor TOPLESS to jasmonate signalling. *Nature* **464**(7289): 788-791.

768 **Plant AR, Larrieu A, Causier B. 2021.** Repressor for hire! The vital roles of TOPLESS-mediated transcriptional repression in plants. *New Phytol*: 10.1111/nph.17428.

770 **Pruitt RN, Zhang L, Saile SC, Karelina D, Fröhlich K, Wan W-L, Rao S, Gust AA, Locci F, Joosten MHAJ, et al. 2020.** *Arabidopsis* cell surface LRR immune receptor signaling through the EDS1-PAD4-ADR1 node. *bioRxiv*: 2020.2011.2023.391516.

773 **Saile SC, Jacob P, Castel B, Jubic LM, Salas-Gonzáles I, Bäcker M, Jones JDG, Dangl JL, El Kasmi F. 2020.** Two unequally redundant "helper" immune receptor families mediate Arabidopsis thaliana intracellular "sensor" immune receptor functions. *PLOS Biology* **18**(9): e3000783.

776 **Shen L, Shao N-Y, Liu X, Maze I, Feng J, Nestler EJ. 2013.** diffReps: Detecting Differential Chromatin Modification Sites from ChIP-seq Data with Biological Replicates. *PLOS ONE* **8**(6): e65598.

778 **Sohn KH, Segonzac C, Rallapalli G, Sarris PF, Woo JY, Williams SJ, Newman TE, Paek KH, Kobe B, Jones JDG. 2014.** The Nuclear Immune Receptor RPS4 Is Required for RRS1^{SLH1}-Dependent Constitutive Defense Activation in *Arabidopsis thaliana*. *PLOS Genetics* **10**(10): e1004655.

781 **Straus MR, Rietz S, Ver Loren van Themaat E, Bartsch M, Parker JE. 2010.** Salicylic acid antagonism of EDS1-driven cell death is important for immune and oxidative stress responses in Arabidopsis. *Plant J* **62**(4): 628-640.

784 **Sun T, Zhang Y, Li Y, Zhang Q, Ding Y, Zhang Y. 2015.** ChIP-seq reveals broad roles of SARD1 and CBP60g in regulating plant immunity. *Nature Communications* **6**(1): 10159.

786 **Sun X, Lapin D, Feehan JM, Stolze SC, Kramer K, Dongus JA, Rzemieniewski J, Blanvillain-Baufumé S, Harzen A, Bautor J, et al. 2021.** Pathogen effector recognition-dependent association of NRG1 with EDS1 and SAG101 in TNL receptor immunity. *Nat Commun* **12**(1): 3335.

789 **Szemenyei H, Hannon M, Long JA. 2008.** TOPLESS Mediates Auxin-Dependent Transcriptional Repression During *Arabidopsis* Embryogenesis. *Science* **319**(5868): 1384-1386.

791 **Tian W, Hou C, Ren Z, Wang C, Zhao F, Dahlbeck D, Hu S, Zhang L, Niu Q, Li L, et al. 2019.** A calmodulin-gated calcium channel links pathogen patterns to plant immunity. *Nature* **572**(7767): 131-135.

793 **Todesco M, Balasubramanian S, Hu TT, Traw MB, Horton M, Epple P, Kuhns C, Sureshkumar S, Schwartz C, Lanz C, et al. 2010.** Natural allelic variation underlying a major fitness trade-off in Arabidopsis thaliana. *Nature* **465**(7298): 632-636.

796 **Tsuda K, Sato M, Stoddard T, Glazebrook J, Katagiri F. 2009.** Network Properties of Robust Immunity in Plants. *PLOS Genetics* **5**(12): e1000772.

798 **Tsuda K, Somssich IE. 2015.** Transcriptional networks in plant immunity. *New Phytologist* **206**(3): 932-947.

799 **van Butselaar T, Van den Ackerveken G. 2020.** Salicylic Acid Steers the Growth-Immunity Tradeoff. *Trends in Plant Science* **25**(6): 566-576.

801 **Van Moerkercke A, Duncan O, Zander M, Šimura J, Broda M, Vanden Bossche R, Lewsey MG, Lama S, Singh KB, Ljung K, et al. 2019.** A MYC2/MYC3/MYC4-dependent transcription factor network regulates water spray-responsive gene expression and jasmonate levels. *Proceedings of the National Academy of Sciences* **116**(46): 23345.

805 **Wagner S, Stuttmann J, Rietz S, Guerois R, Brunstein E, Bautor J, Niefind K, Parker JE. 2013.** Structural Basis for Signaling by Exclusive EDS1 Heteromeric Complexes with SAG101 or PAD4 in Plant Innate Immunity. *Cell Host & Microbe* **14**(6): 619-630.

808 **Walters DR. 2015a.** Growth, Development and Yield of Infected and Infested Plants and Crops. *Physiological Responses of Plants to Attack*: 24-40.

810 **Walters DR. 2015b.** Photosynthesis in Attacked Plants and Crops. *Physiological Responses of Plants to Attack*: 41-87.

812 **Wang H, Li S, Li Ya, Xu Y, Wang Y, Zhang R, Sun W, Chen Q, Wang X-j, Li C, et al. 2019.** MED25 connects enhancer–promoter looping and MYC2-dependent activation of jasmonate signalling. *Nature Plants* **5**(6): 616-625.

Wildermuth MC, Dewdney J, Wu G, Ausubel FM. 2001. Isochorismate synthase is required to synthesize salicylic acid for plant defence. *Nature* **414**(6863): 562-565.

Yang L, Teixeira PJPL, Biswas S, Finkel OM, He Y, Salas-Gonzalez I, English ME, Epple P, Mieczkowski P, Dangl JL. 2017. Pseudomonas syringae Type III Effector HopBB1 Promotes Host Transcriptional Repressor Degradation to Regulate Phytohormone Responses and Virulence. *Cell Host & Microbe* **21**(2): 156-168.

Yu A, Lepère G, Jay F, Wang J, Bapaume L, Wang Y, Abraham A-L, Penterman J, Fischer RL, Voinnet O, et al. 2013. Dynamics and biological relevance of DNA demethylation in *Arabidopsis* antibacterial defense. *Proceedings of the National Academy of Sciences* **110**(6): 2389-2394.

Yu C-P, Lin J-J, Li W-H. 2016. Positional distribution of transcription factor binding sites in Arabidopsis thaliana. *Scientific Reports* **6**(1): 25164.

Yuan M, Jiang Z, Bi G, Nomura K, Liu M, Wang Y, Cai B, Zhou J-M, He SY, Xin X-F. 2021. Pattern-recognition receptors are required for NLR-mediated plant immunity. *Nature* **592**(7852): 105-109.

Zander M, Lewsey MG, Clark NM, Yin L, Bartlett A, Saldierna Guzmán JP, Hann E, Langford AE, Jow B, Wise A, et al. 2020. Integrated multi-omics framework of the plant response to jasmonic acid. *Nature Plants* **6**(3): 290-302.

Zavaliev R, Mohan R, Chen T, Dong X. 2020. Formation of NPR1 Condensates Promotes Cell Survival during the Plant Immune Response. *Cell* **182**(5): 1093-1108.e1018.

Zervudacki J, Yu A, Amesefe D, Wang J, Drouaud J, Navarro L, Deleris A. 2018. Transcriptional control and exploitation of an immune-responsive family of plant retrotransposons. *The EMBO Journal* **37**(14): e98482.

Zhang Y, Goritschnig S, Dong X, Li X. 2003. A gain-of-function mutation in a plant disease resistance gene leads to constitutive activation of downstream signal transduction pathways in suppressor of npr1-1, constitutive 1. *The Plant Cell* **15**(11): 2636-2646.

Zhang Y, Song G, Lal NK, Nagalakshmi U, Li Y, Zheng W, Huang P-j, Branon TC, Ting AY, Walley JW, et al. 2019. TurboID-based proximity labeling reveals that UBR7 is a regulator of N NLR immune receptor-mediated immunity. *Nature Communications* **10**(1): 3252.

Zhang Y, Xu S, Ding P, Wang D, Cheng YT, He J, Gao M, Xu F, Li Y, Zhu Z, et al. 2010. Control of salicylic acid synthesis and systemic acquired resistance by two members of a plant-specific family of transcription factors. *Proceedings of the National Academy of Sciences* **107**(42): 18220-18225.

Zheng X-y, Spivey NW, Zeng W, Liu P-P, Fu ZQ, Klessig DF, He SY, Dong X. 2012. Coronatine Promotes *Pseudomonas syringae* Virulence in Plants by Activating a Signaling Cascade that Inhibits Salicylic Acid Accumulation. *Cell Host & Microbe* **11**(6): 587-596.

Zhou M, Lu Y, Bethke G, Harrison BT, Hatsugai N, Katagiri F, Glazebrook J. 2018. WRKY70 prevents axenic activation of plant immunity by direct repression of SARD1. *New Phytologist* **217**(2): 700-712.

Zhu Z, Xu F, Zhang Y, Cheng YT, Wiermer M, Li X, Zhang Y. 2010. Arabidopsis resistance protein SNC1 activates immune responses through association with a transcriptional corepressor. *Proceedings of the National Academy of Sciences* **107**(31): 13960-13965.